Progress In Electromagnetics Research C, Vol. 116, 51–64, 2021

Design and Experimental Validation of UWB MIMO Antenna with Triple Band-Notched Characteristics

Muhammad K. Khan and Quanyuan Feng*

Abstract—A compact pot-shaped Multiple Input Multiple Output (MIMO) Antenna with triple notched band characteristics is presented for Ultra Wide Band (UWB) applications. The comprehensive dimension of the presented antenna is $17 \times 32\,\text{mm}^2$. The presented antenna has two identical pot-shaped radiators, 7-shaped stubs, T-shaped strips, M- and C-shaped slots. Two novel 7-shaped stubs are connected to the antenna ground plane to obtain -22 dB enhanced isolation. The presented antenna works from 2.95 to 12.1 GHz with triple stopped WiMAX, WLAN, and X bands. A novel T-shaped strip is connected to the antenna ground plane to stop the WiMAX band (3.3–4.4) GHz. C- and M-shaped slots are etched in the antenna radiators to stop WLAN (5.20–6.12) GHz and X (7.6–8.15) GHz bands, respectively. The peak gain of the proposed antenna is from 1.5 to 5 dB with a radiation efficiency of 80–90%. The Envelope Correlation Coefficient (ECC) of the proposed antenna is less than 0.01 with a Diversity Gain greater than 9.99 except for the notched bands.

1. INTRODUCTION

In the recent past, UWB Technology got tremendous response from researchers due to its reliable communication, wide frequency spectrum, and high data rate [1]. Among all these great advantages, conventional UWB technology suffers from the problems of multipath fading and high bit error rate, which can minimize the system performance [2]. To address the limitation of UWB technology, the MIMO system will enhance the system channel capacity and reliability without using extra bandwidth and additional power [3]. By combining the MIMO system with UWB technology, different antenna shapes are designed in [4–6]. Placing antennas radiating elements in a tiny space will create a high mutual coupling problem. To overcome the problem of mutual coupling, different decoupling structures are designed in [7–10]. UWB system also has some electromagnetic interference with coexisting narrow bands, thus different notch structures are presented to stop this interference [11–23].

A UWB antenna with E and F slots is presented for UWB application in [11]. The antenna size is $17 \times 13\,\text{mm}^2$. The operating frequency of the proposed antenna is from 2.38 to 10.41 GHz with dual stopbands of 2.68–3.55 GHz and 4.5–5.8 GHz. The stopbands are achieved by creating E-shaped slots in the radiator. A novel switchable antenna having band-notched and switchable functions is proposed in [12]. The compact size of the antenna is $19.5 \times 17\,\text{mm}^2$. The operating bandwidth of the antenna is 3.08–14 GHz with a notched band of 4.87–6.08 GHz. In article [13], an octagonal-shaped antenna having the dual stopband ability is presented. The compact size of the two ports antenna is $19 \times 30\,\text{mm}^2$. The antenna operates from 3.1 to 10.6 GHz, and the two stopbands are obtained by engraving open-ended slots in the radiators. The improved -18 dB isolation is secured by joining a T-structured stub to the antenna ground plane. In article [14], a CPW-fed flexible MIMO antenna having a WiMAX stopband is recommended for WBAN uses. The submitted antenna works from 2.4 to 11.3 GHz. An F-Shaped branch is used to achieve enhanced port isolation. A rectangle-shaped

Received 10 August 2021, Accepted 24 September 2021, Scheduled 10 October 2021
* Corresponding author: Quanyuan Feng (fengquanyuan@163.com).
The authors are with the School of Information Science and Technology, Southwest Jiaotong University, Chengdu 611756, China.

antenna having quadruple stopbands applications is designed in [15]. The presented antenna dimensions are $39 \times 30\,\text{mm}^2$ with an operating bandwidth varying from 3 to 11 GHz. The desired notched bands are gained by utilizing compact U-shaped slots in antenna ground and radiators. The -20 dB mutual coupling is obtained by adding an I-shaped stub to the presented antenna ground plane. A $46 \times 32\,\text{mm}^2$ size novel MIMO UWB antenna having dual stopband properties is proposed in [16]. The antenna working bandwidth is 3–16 GHz with two stopbands obtained by the cup branches technique. To secure -20 dB isolation, repeated strip branches are used on the backside of the antenna.

In article [17], a UWB MIMO Sierpinski Koch antenna is fabricated for UWB properties. The antenna working bandwidth is from 2.5 to 11 GHz having a WLAN notched band. The WLAN stopband is attained by a U-structured slot etched in the designed antenna radiator. The -20 dB enhanced isolation is attained by adding a compact I-shaped stub to the antenna ground. An asymmetrical cup-shaped MIMO antenna having UWB communication properties is designed in [18]. The antenna operating bandwidth is from 3.1 to 11 GHz having a WLAN notched band. To attain the WLAN notched band, a C-shaped slot in a cup-shaped radiator is engraved. The -18 dB enhanced isolation is achieved by introducing an H-slot and a vertical stub. The antenna comprehensive size is $29 \times 40\,\text{mm}^2$. A UWB system with a suspended line technique is presented for MIMO applications in [19]. The antenna compact size is $20 \times 36\,\text{mm}^2$ with operating bandwidth ranging from 3.1 to 11.5 GHz. The WLAN and X notched-bands are obtained by placing an elliptical SRR adjacent to the feed line and a Y-shaped strip within the radiators. Planer Suspended Line (PSL) is used to secure the antenna isolation of -21 dB. A miniaturized Vivaldi antenna with the ability of dual-band rejection is put forward for UWB purposes in [20]. The submitted antenna working bandwidth is 2.5 to 12 GHz with two rejected bands ranging from 5.1 to 5.7 GHz and 6.6 to 7.1 GHz. The antenna comprehensive dimensions are $26 \times 24.5\,\text{mm}^2$ with enhanced isolation of -15 dB.

A MIMO antenna having triple stopband characteristics is recommended in [21]. The designed antenna is $21 \times 36\,\text{mm}^2$ in size. The three notched bands are achieved by using a TVC-EBG structure. The antenna operates from 2 to 11 GHz with -15 dB enhanced isolation. Two L-shaped stubs are utilized to secure enhanced isolation. A two ports CPW-fed MIMO antenna having triple-stopband characteristics are submitted in [22]. The designed intended antenna operates from 2.7 to 11.2 GHz. Fractal defected in the ground, parasitic semi-fractal Koch elements, and fractal resonators are used to stop WiMAX, WLAN, and X bands. The compact antenna size is $30.75 \times 37.80\,\text{mm}^2$ with -20 dB enhanced isolation. A MIMO antenna having a counter faced C-shaped structure is designed for UWB communications in [23]. The $20 \times 34\,\text{mm}^2$ size antenna working bandwidth is 3.10–10.60 GHz except for the stopbands. The three stopbands are secured by engraving an inverted U-shaped slot in the antenna radiator and also on the antenna feed line. Another line slot is engraved on the designed antenna ground plane for the third notched band. The -20 dB improved isolation is attained by applying a loaded stub to the antenna ground structure.

In this proposed research work, a novel pot-shaped UWB MIMO antenna with triple notched band characteristics for WiMAX, WLAN, and X bands is presented. The UWB spectrum is achieved by two pot-shaped radiating components with a microstrip fed line. Two 7-shaped stubs are attached to the ground plane to enhance the isolation to -22 dB. The dimensions of the designed antenna are $17 \times 32\,\text{mm}^2$ with working bandwidth ranging from 2.95 to 12.1 GHz. A T-shaped strip is connected to the ground plane to stop the (3.3–4.4) GHz WiMAX band. A C-shaped slot is etched in the pot-shaped radiator to stop the WLAN band (5.20–6.12) GHz. Another M-shaped novel slot is slotted in the radiator to stop the (7.6–8.15) GHz X band. The proposed antenna is examined and simulated in Computer Simulation Technology (CST) Microwave Studio.

2. ANTENNA DESIGN MODEL

In the first step, the radius of the circle is determined by the following equation [24].

$$a = \frac{F}{\left\{1 + \dfrac{2h}{\pi\varepsilon_r F}\left[\ln\left(\dfrac{\pi F}{2h}\right) + 1.7726\right]\right\}^{\frac{1}{2}}} \tag{1}$$

where F is given by

$$F = \frac{8.791 \times 10^9}{f_r\sqrt{\varepsilon_r}}$$

Here, ε_r is the dielectric constant of the substrate, h the height of the substrate, and f_r the resonant frequency. After the parametric study, the radius of the circle and elliptical shapes is optimized in such a way that the proposed antenna achieves the entire UWB spectrum. After optimizing the dimensions of circle, ellipse, ground, strips, and slots, the recommended antenna detail dimensions are given in millimeters and expressed in Table 1.

Table 1. The designed MIMO antenna detail dimensions in millimeters.

Parameters	Size (mm)	Parameters	Size (mm)
W	32	L	17
$W1$	1.3	$L1$	4.74
$R1$	2.15	$R2$	2.4
m	2.5	$m1$	2.3
$m2$	0.3	$c1$	2.5
$c2$	2.7	$c3$	6.4
G	3.5	Gs	3.25
Gw	14	Is	2
Iw	14	T	11
$t1$	8.5	$t2$	0.25
$t3$	5.8	u	0.3

The front and back sides of the presented antenna are given in Figure 1. The presented antenna is fabricated on an FR4 substrate with dielectric constant 4.4, loss tangent 0.02, and thickness 1.6 mm. The comprehensive size of the recommended antenna is $17 \times 32\,\text{mm}^2$. The designed antenna has two pot-shaped radiators, two T-shaped strips, a ground plane with 7-shaped stubs, M- and C-shaped slots in radiating patches. The proposed antenna radiator consists of a half-circle, an ellipse, and a small rectangle. The $50\,\Omega$ microstrip line feeds the radiating elements with dimension $W1 \times L1$. Two 7-shaped stubs to the antenna ground plane are added to attain -22 dB enhanced isolation. A novel T-shaped strip is introduced from the ground to stop the (3.3–4.4) GHz WiMAX band. A C-shaped slot is etched in the pot-shaped radiator to stop the WLAN band (5.2–6.12) GHz. Another novel M-shape in the designed antenna radiator is slotted to stop X band (7.6–8.15) GHz.

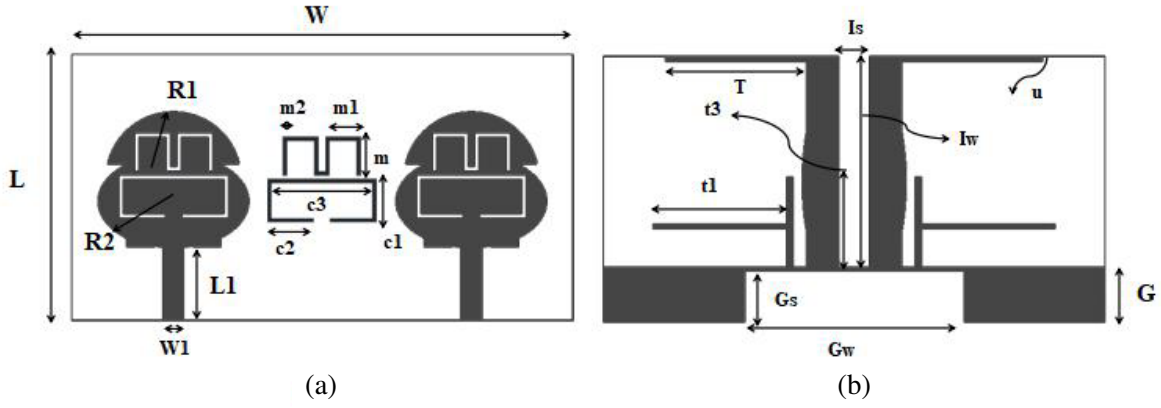

Figure 1. The designed antenna, (a) top view and (b) bottom view.

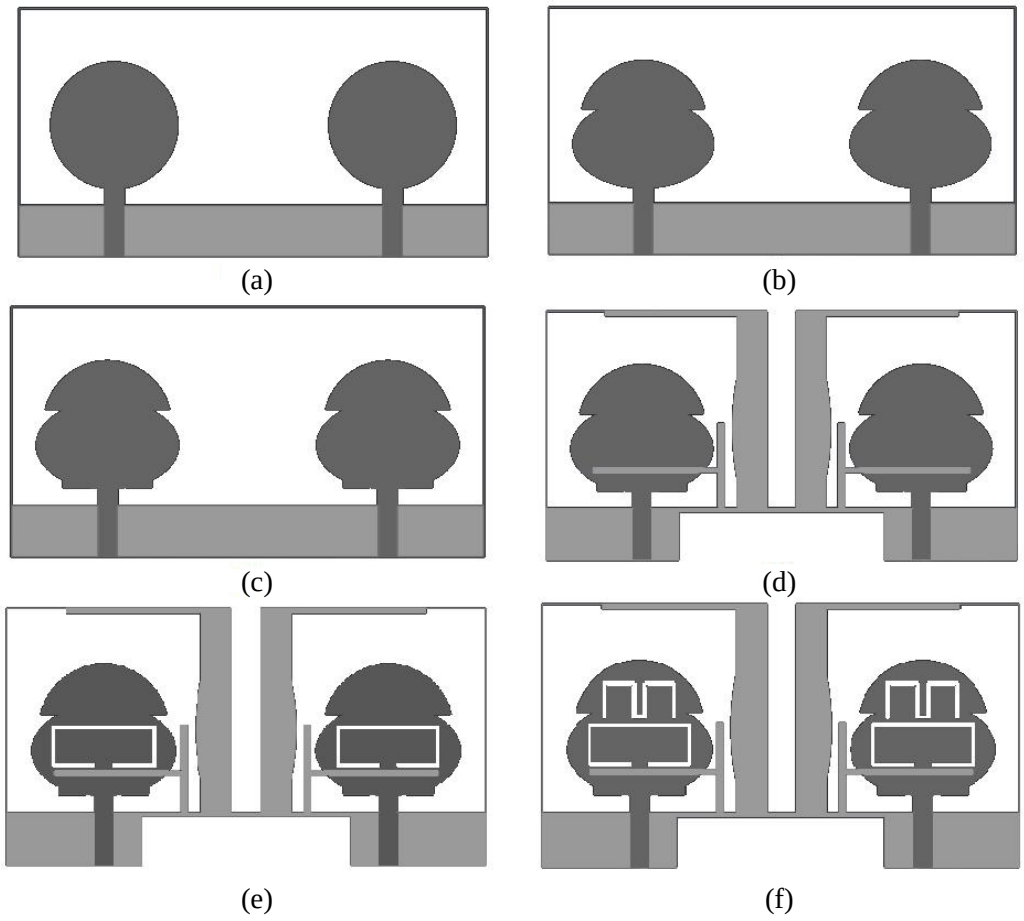

Figure 2. Stepwise designing of proposed MIMO antenna. (a) Circle-shaped antenna, (b) half circular-elliptical shaped antenna, (c) Pot-shaped antenna without strips and stubs, (d) Pot-shaped antenna having T-shaped strip and 7-shaped stubs, (e) Pot-shaped antenna with T-shaped strip and C-shaped slots, and (f) Pot-shaped antenna having T-shaped strip, C and M-shaped slots.

To understand the design model further several antenna structures are simulated and examined in CST Microwave Studio as given in Figure 2.

In the first step, a circle-shaped antenna fed by a microstrip line is designed, and the results are examined. The circle-shaped antenna works from 4.5 to 14.5 GHz as clear from Figure 3. To obtain the entire UWB spectrum, the circle-shaped antenna is modified to a half circle-ellipse shaped antenna. The half circular-elliptical antenna operates from 4.3 to 14.5 GHz. A further modification is needed to achieve the entire UWB spectrum. The half circular-elliptical antenna is modified to a pot-shaped antenna, and it is clear from Figure 3 that the proposed antenna covers the entire UWB spectrum. In the next step, a 7-shaped stub and a T-shaped strip are added to the ground plane to obtain the notched WiMAX band. It is clear from Figure 3 that the pot-shaped antenna having the novel T-shaped strip operates from 2.95–12.1 GHz with a notched WiMAX band (3.3–4.4) GHz. To stop the WLAN band, a C-shaped slot is etched in the pot-shaped radiator to attain the WLAN band (5.2–6.12) GHz as clear from Figure 3. An M-shaped slot is slotted in the radiator to obtain X band (7.6–8.15) GHz as clear from Figure 3.

To obtain the reduced mutual coupling, the evolution process of the 7-shaped stub is given in Figure 4. In the first step, the proposed pot-shaped antenna with the conventional ground is designed, and the results are examined in terms of mutual coupling. It is clear from Figure 5 that the mutual coupling between the two ports of the antenna is -12 dB.

To reduce the mutual coupling further, a vertical stub is added to the conventional ground plane,

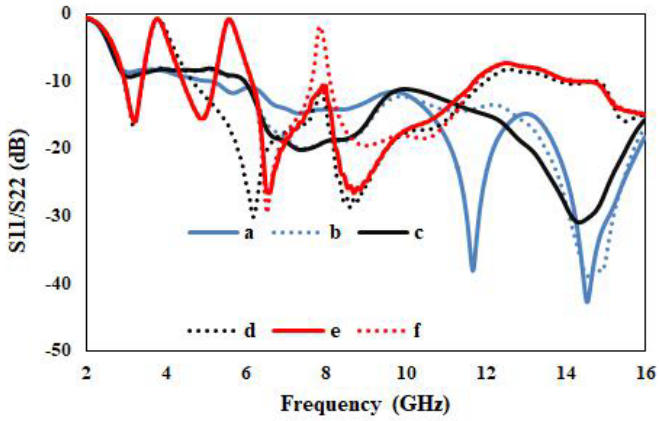

Figure 3. S_{11}/S_{22} for different design models. (a) Circle-shaped antenna, (b) half circular-elliptical shaped antenna, (c) Pot-shaped antenna without strips and stubs, (d) Pot-shaped antenna having T-shaped strip and 7-shaped stubs, (e) Pot-shaped antenna with T-shaped strip and C-shaped slots, and (f) Pot-shaped antenna having T-shaped strip, C and M-shaped slots.

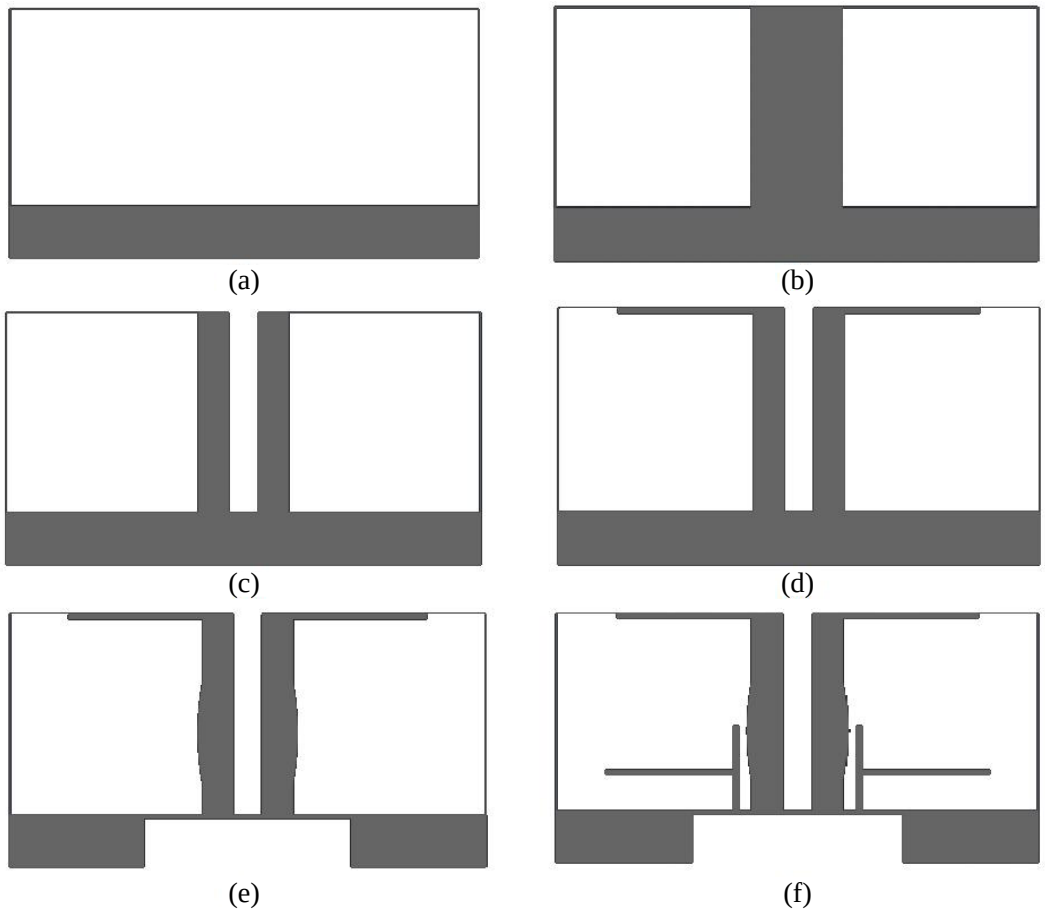

Figure 4. Stepwise designing of stub structure of the designed MIMO antenna. (a) Conventional ground, (b) conventional ground with a vertical stub, (c) I-shaped stubs, (d) 7-shaped stubs, (e) 7-shaped stubs with ground slot, and (f) 7-shaped stubs with ground slot and T-shaped strips.

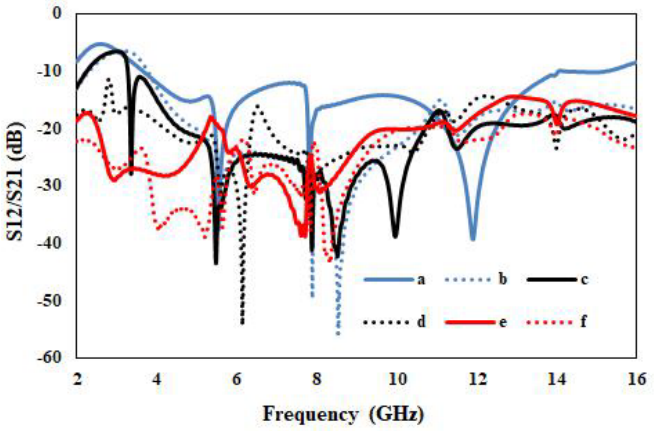

Figure 5. S_{12}/S_{21} of proposed MIMO antenna for different stub structures. (a) Conventional ground, (b) conventional ground with a vertical stub, (c) I-shaped stubs, (d) 7-shaped stubs, (e) 7-shaped stubs with ground slot, and (f) 7-shaped stubs with ground slot and T-shaped strips.

and the results with the I-shaped stub are examined. It is clear from Figure 5 that the mutual coupling is reduced to −15 dB. A slot is etched in vertical stub for modification to I-shaped stubs, and results for the two I-shaped stubs are examined. It is clear from Figure 5 that the mutual coupling is reduced further but not to the desired range at lower frequencies. To achieve the desired reduced mutual coupling, the two I-shaped stubs are modified to 7-shaped stubs, and the results for the 7-shaped stubs confirm that the mutual coupling is reduced to −17 dB at the lower frequencies. To obtain the desirable reduced mutual coupling, two vertical half ellipses are added to the outer sides of the I-shaped stubs, and a slot is etched in the antenna ground plane. It is clear from Figure 5 that the antenna desired mutual coupling is reduced to −22 dB. In the last step, the T-shaped strip effect on the antenna mutual coupling is examined. It is clear from Figure 5 that the mutual coupling of the proposed antenna is not affected, and it is −22 dB in the entire UWB range, which is the desired reduced mutual coupling for the designed antenna.

The UWB antenna obtains a wide bandwidth that overlaps with existing narrow bands that lie in the UWB range such as WiMAX, WLAN, and X bands. To stop this electromagnetic interference between the UWB system and these narrow bands, a T-shaped strip, C- and M-shaped slots are proposed in the current work. To obtain the notched WiMAX band, novel T-shaped strips are connected to the ground plane. A C-shaped slot is etched in the pot-shaped radiator to stop the WLAN band. To stop the X band, another M-shaped slot is slotted in the designed antenna radiators. The novel T-shaped strip, C-shaped slot, and M-shaped slot dimensions are optimized in such a way so that the desired UWB performance and notched frequencies individual performances are not affected. To obtain the desired notched frequencies, the dimensions of strips are calculated using Equation (1), and slots dimensions are calculated from Equation (2) [1].

$$L = \frac{c}{4f_n\sqrt{(\varepsilon_r + 1)/2}} \tag{2}$$

$$L = \frac{c}{2f_n\sqrt{(\varepsilon_r + 1)/2}} \tag{3}$$

In the above equation, (L) is the length of the slot and strip at the notched frequency (f_n), (c) the speed of light, and (ε_r) the relative permittivity of the antenna substrate.

To analyze the proposed antenna further, the current distribution of the proposed antenna is investigated and analyzed at different frequencies 3.8, 5.6, and 7.85 GHz. It is clear from Figure 6 that with the conventional ground at frequencies 3.8, 5.6, and 7.85 GHz, a strong surface current is observed at port 2 of the antenna which results in strong mutual coupling between the two ports. To minimize the strong mutual coupling between two ports, a 7-shaped stub is added to the ground plane. After adding the 7-shaped stub and T-shaped strip to the designed antenna ground, results are examined at

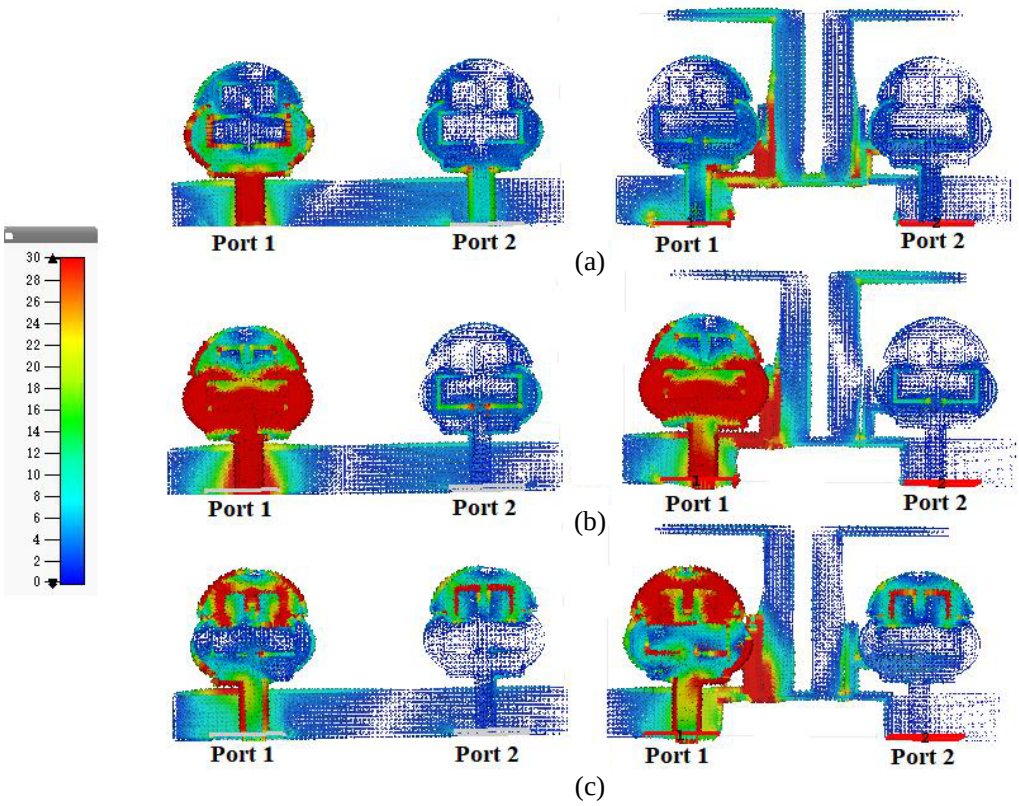

Figure 6. Surface current distribution for conventional ground and 7-shaped stubs for various frequencies (a) 3.8, (b) 5.6 and (c) 7.85 GHz.

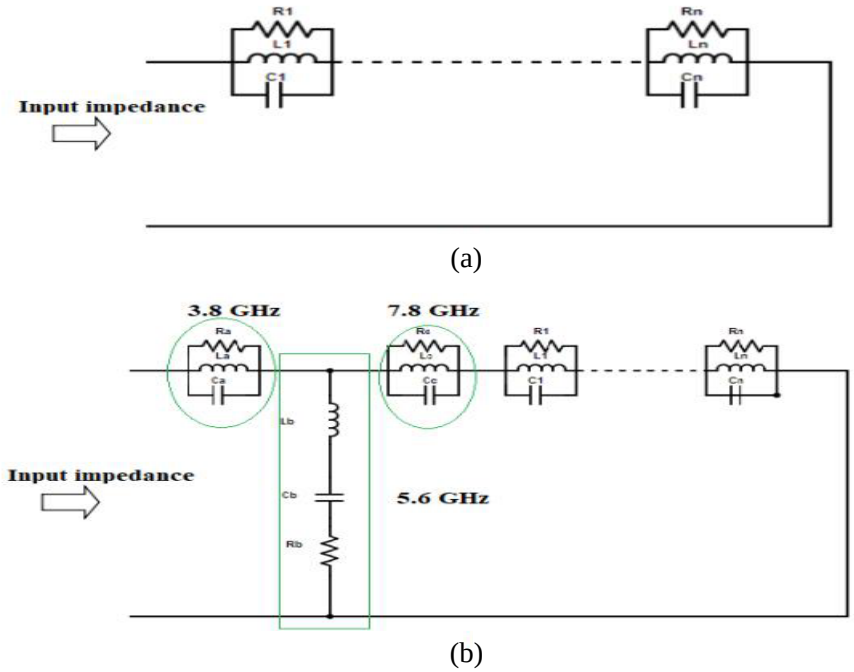

Figure 7. Equivalent circuit of the designed antenna. (a) UWB antenna and (b) proposed triple notched UWB antenna.

frequencies 3.8, 5.6, and 7.85 GHz, and it is clear from Figure 6 that the surface current concentrates at port 1, 7-shaped stub, and the T-shaped strip which results in a sharp WiMAX stopband. The mutual current at port 2 is minimized. At frequency 5.6 GHz, the surface current is observed and examined after engraving the C-shaped slot in the antenna radiator, and it is clear from Figure 6 that after adding the stub the surface current concentrates at port 1, 7-shaped stub, and C-shaped slot which results in a sharp WLAN stopband. After examining the surface current at frequency 7.85, it is clear from Figure 6 that when the proposed stub is added to the antenna, the current concentrates at port 1, stub, and M-shaped slot, which results in a sharp notched X band and enhanced isolation.

For a narrow band microstrip antenna, an equivalent circuit is represented by a parallel RLC circuit [24]. To design a UWB antenna, a wide bandwidth is taken into consideration. The UWB antenna is not considered as a single resonance but multiple overlapping resonances. Thus the UWB antennas equivalent circuit is presented by a series of parallel RLC resonators as shown in Figure 7(a). The band-stop components are given with two parallel and one series RLC resonators connected to the UWB antenna. The T-shaped strip and M-shaped slot are represented by parallel RLC resonators. The high impedance due to the T-shaped strip and M-shaped slot causes to reflect back the maximum power to the input terminal which rejects the frequencies of WiMAX and X bands. The C-shaped slot is represented by the series RLC element which acts as a short circuit, and the maximum amount of input power returns back to input terminal which causes the stopped WLAN band.

3. RESULTS AND DISCUSSIONS

The designed pot-shaped antenna with a 7-shaped stub is printed on an FR4 substrate with a thickness of 1.6 mm. The dielectric constant of FR4 is 4.4, and the loss tangent is 0.02. The FR4 substrate is easily available commercially. The fabricated front and back views of the proposed pot-shaped antenna are given in Figure 8.

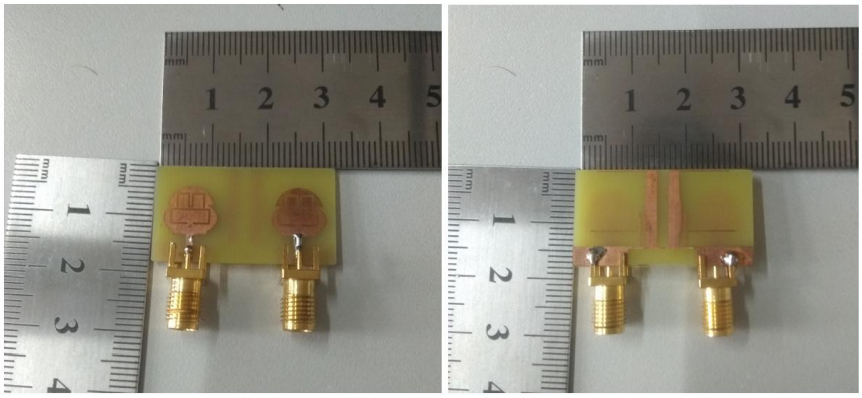

Figure 8. Fabricated prototype of the designed MIMO antenna.

3.1. Reflection Coefficient

To inspect the antenna performance further, the dimensions based antenna is fabricated, and the results are measured. Measured results of the designed antenna are compared with simulated ones in Figure 9. It clearly shows that measured and simulated results have a good agreement with one another.

The simulated and measured results show that the suggested antenna operates from 2.95–12.1 GHz with notches from 3.3–4.4 GHz, 5.2–6.12 GHz, and 7.6–8.15 GHz for WiMAX, WLAN, and X bands, respectively. The WiMAX notched band (3.3–4.4) GHz is obtained by adding a novel T-shaped strip to the ground plane. A C-shaped slot in the radiator is etched to stop the WLAN band (5.2–6.12) GHz. Another novel M-shaped slot is slotted in a pot-shaped radiator to stop the X band (7.6–8.15) GHz. The obtained measured and simulated isolation is greater than -22 dB, and it is achieved by adding a 7-shaped stub and a ground slot to the proposed antenna.

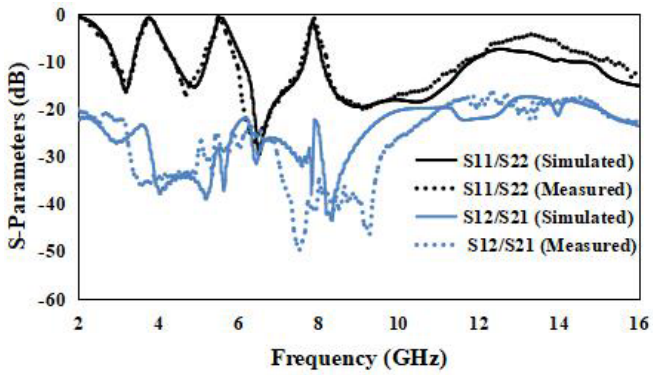

Figure 9. Simulated and measured S-parameters of the proposed antenna.

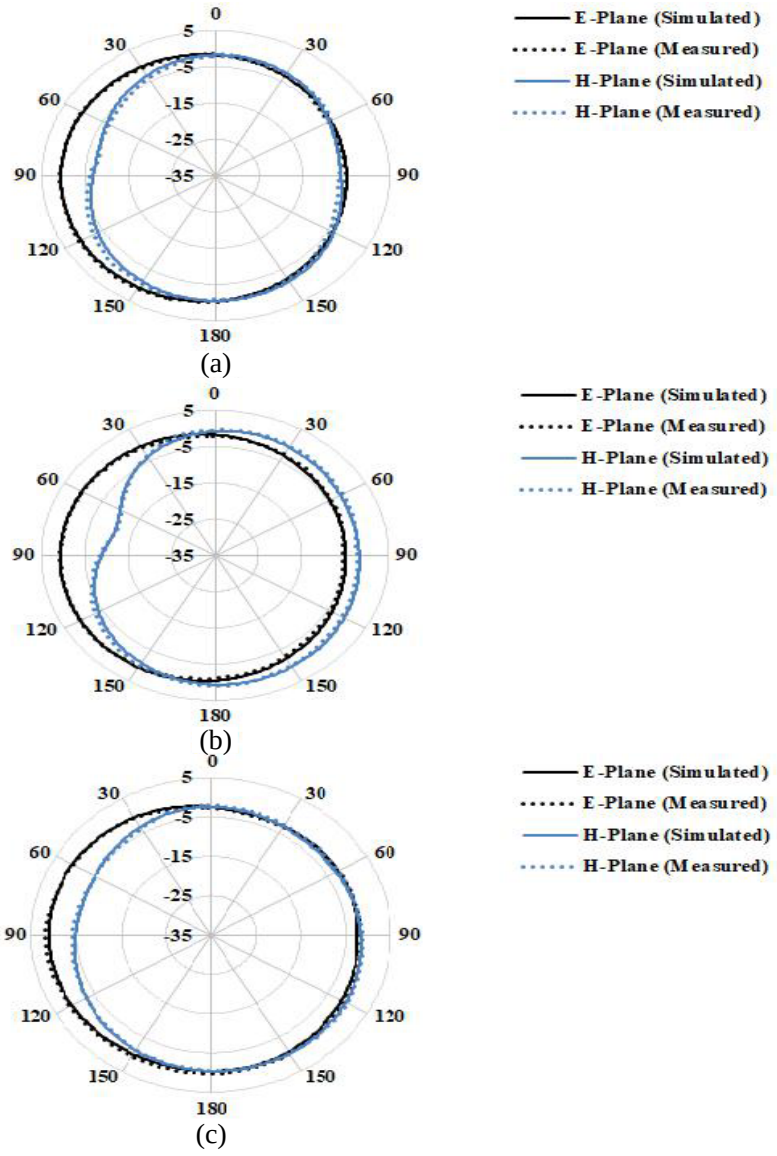

Figure 10. Simulated and measured radiation patterns of proposed antenna at (a) 5 GHz, (b) 7 GHz and (c) 9 GHz.

3.2. Radiation Patterns, Radiation Efficiency and Peak Gain

To validate the proposed antenna further, radiation patterns, radiation efficiency, 3D gain, and peak gain of the proposed antenna are studied in this section. The simulated and measured radiation patterns of the proposed antenna are given in Figure 10, and it is clear from Figure 10 that a good agreement is found between simulated and measured results. To analyze and study the radiation properties further, the designed antenna is tested in an anechoic chamber. The proposed antenna performances are tested at 5, 7, and 9 GHz. The measured results at these frequencies are stable and omnidirectional. Port 1 of the proposed antenna is excited and port 2 terminated. For identical radiating components, the results with port 2 are mirror images with that of port 1 with a 90° rotation.

The co- and cross-polarizations at E- and H-planes are given in Figure 11. The co- and cross-polarizations at both E- and H-planes are nearly omnidirectional. The omnidirectional radiation patterns help to prevent coming signal dropout irrespective of the direction of arrival. The result of co-polarization is greater than cross-polarization as clear from Figure 11.

The 3D gain of the proposed antenna is given in Figure 12. It is clear from Figure 12 that the 3D gains are −5.16 dB at 3.8 GHz and −4.7 dB at 5.6 GHz notched frequencies. The gain of the proposed

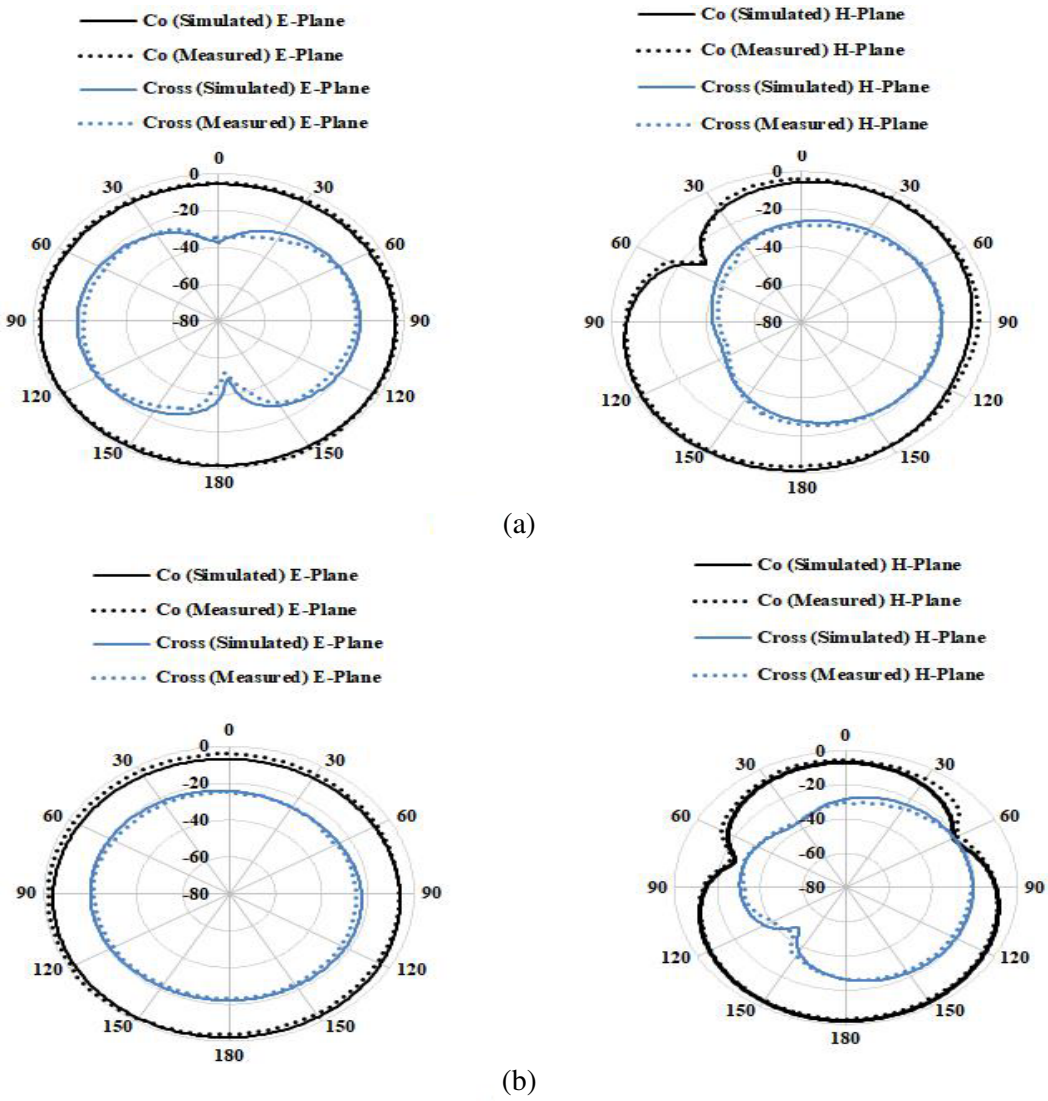

Figure 11. Simulated and measured co and cross polarization of proposed antenna at (a) 5 GHz and (b) 9 GHz.

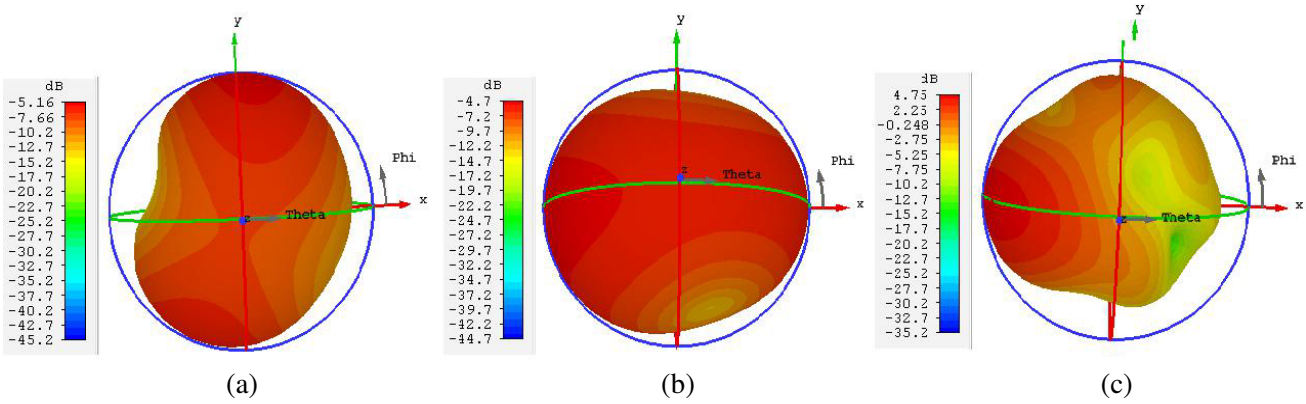

(a) (b) (c)

Figure 12. 3D gain of the proposed antenna (a) 3.8 GHz, (b) 5.6 GHz, and (c) 10 GHz.

antenna is 4.75 dB at 10 GHz.

Another essential parameter for the MIMO antenna to examine is peak gain. The peak gain is from 1.5 to 5 dB except for the notched band as shown in Figure 13. The radiation efficiency of the proposed antenna is from 80 to 90% except for the three stopbands.

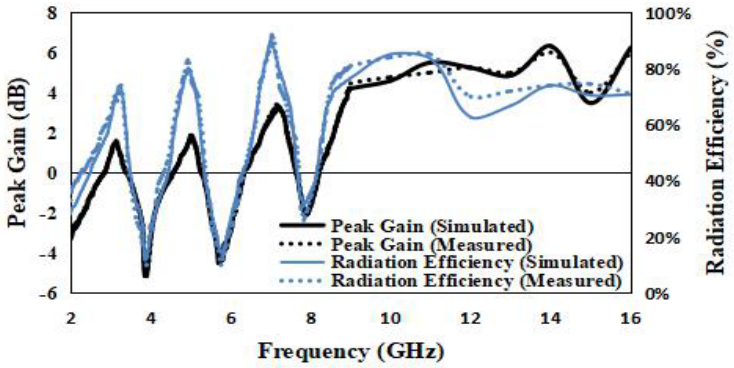

Figure 13. Gain and radiation efficiency of the designed antenna.

3.3. Diversity Performances of the Recommended MIMO Antenna

To examine and study the suggested antenna further, the designed antenna is examined in terms of diversity performances. The practical limit for ECC is 0.5, and it is calculated from the following two equations [25]. For loss free antennas, the ECC is calculated with both S-parameters and radiation patterns. As clear from Figure 13, the proposed antenna efficiency is from 80 to 90%. The ECC of the proposed antenna is calculated using Equation (5).

$$\mathrm{ECC} = \frac{\left|S_{11}^{*}S_{12} + S_{21}^{*}S_{22}\right|^{2}}{\left(1 - |S_{11}|^{2} - |S_{21}|^{2}\right)\left(1 - |S_{22}|^{2} - |S_{12}|^{2}\right)} \tag{4}$$

$$\mathrm{ECC} = \frac{\left|\iint\limits_{4\pi}\left[\vec{F}_1(\theta,\phi)\cdot\vec{F}_2(\theta,\phi)\right]d\Omega\right|^{2}}{\iint\limits_{4\pi}\left|\vec{F}_1(\theta,\phi)\right|^{2}d\Omega\iint\limits_{4\pi}\left|\vec{F}_2(\theta,\phi)\right|^{2}d\Omega} \tag{5}$$

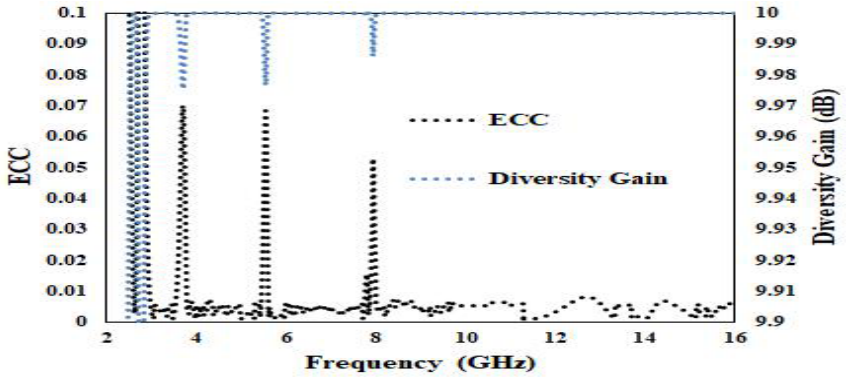

Figure 14. The designed antenna ECC and Diversity Gain results.

Table 2. Comparison of recommended design with designs in the literature.

Ref. #	Size (mm^2)	Operating frequency (GHz)	Notched bands (GHz)	Mutual coupling (dB)	Gain (dB)	Radiation Efficiency (%)	ECC
[13]	19×30	3.1–10.6	4.37–5.95, 6.52–7.45	-18	1.2–2.91	70–90	0.13
[14]	30×56.5	2.4–11.3	3.1–4.3	-23	5.35	-	0.008
[15]	39×30	3–11	5.2–5.51, 6.1–6.53, 7.37–7.8, 9.15–9.7	-20	1.6–5.8	-	0.02
[16]	46×32	3–16	5.15–5.825, 7–7.8	-20	4	-	0.1
[17]	40×20	2.5–11	5–6	< -20	3	-	< 0.1
[18]	29×40	3.1–11	5.725–5.825	< -18	2–4.9	80–92	0.0005
[19]	20×36	3.1–11.5	5.45–5.85, 7.15–7.95	< -21	1.8–3	60–85	< 0.19
[20]	26×24.5	2.5–12	5.1–5.9, 6.6–7.1	< -15	-	> 60	0.02
[21]	21×36	2–11	3.3–3.7, 5–6, 7.9–8.4	-15	-7	80	0.015
[22]	30.75×37.80	2.7–11.22	3.7–4.2, 5.15–5.825, 7.9–8.4	-20	0.07–3.4	52–72	0.035
[23]	20×34	3.1–10.6	3.51–4.3, 5.5–5.6, 8.4–8.8	< -20	2–4	81	0.2
Proposed work	17×32	2.95–12.1	3.3–4.4, 5.2–6.12, 7.6–8.15	-22	1.5–5	80–90	0.01

$\vec{F}_1(\theta, \phi)$ is the field radiation pattern of port 1, $\vec{F}_2(\theta, \phi)$ the field radiation pattern of port 2, and $\cdot$ the Hermitian product. Diversity gain of the MIMO antenna is measured from Equation (6).

$$\mathrm{DG} = 10\sqrt{1 - (\mathrm{ECC})^2} \tag{6}$$

The ECC of the proposed antenna is less than 0.01 except for notched bands. The ECCs at stopbands are 0.07 at 3.8 GHz, 0.068 at 5.6 GHz, and 0.052 at 7.85 GHz. The recommended antenna diversity gain is greater than 9.99 dB except for notched bands. The diversity gains at notched frequencies are 9.97 dB at 3.8 GHz, 9.976 dB at 5.6 GHz, and 9.98 dB at 7.85 GHz as shown in Figure 14. A detailed comparison of the presented design with the designs in literature is conducted in Table 2.

4. CONCLUSIONS

A two ports pot-shaped MIMO antenna is presented for UWB applications with triple-notched band characteristics for WiMAX, WLAN, and X bands. Two 7-shaped stubs with a ground slot are used to improve isolation to desirable −22 dB. All antenna performances such as return loss, radiation patterns, mutual coupling, peak gain, radiation efficiency, ECC, and diversity gain are all within appropriate limits in the whole UWB range. These performances make the planned antenna an advisable candidate for the UWB MIMO system with triple notched band characteristics.

ACKNOWLEDGMENT

This work is supported by Key Project of the National Natural Science Foundation of China under Grants 62090012, 62031016, 61831017 and the Sichuan Provincial Science and Technology Important Projects under Grants 2019YFG0498, 2020YFG0282, 2020YFG0452, and 2020YFG0028.

REFERENCES

1. Khan, M. I., M. I. Khattak, G. Witjaksono, Z. U. Barki, S. Ullah, I. Khan, and B. M. Lee, "Experimental investigation of a planar antenna with band rejection features for ultra-wide band (UWB) wireless networks," *International Journal of Antennas and Propagation*, Vol. 2019, Art no. 2164716, 2019.
2. Chen, Z., W. Zhou, and J. Hong, "A miniaturized MIMO antenna with triple band-notched characteristics for UWB applications," *IEEE Access*, Vol. 9, 63646–63655, 2021.
3. Iqbal, A., U. A. Saraereh, A. W. Ahmed, and S. Bashir, "Mutual coupling reduction using F-shaped stubs in UWB-MIMO antenna," *IEEE Access*, Vol. 6, 2755–2759, 2018.
4. Zhang, J. Y., F. Zhang, W. P. Tian, and Y. L. Luo, "ACS-fed UWB-MIMO antenna with shared radiator," *Electronics Letters*, Vol. 51, No. 17, 1301–1302, 2015.
5. Roshna, T. K., U. Deepak, V. R. Sajitha, K. Vasudeven, and P. Mohan, "A compact UWB MIMO antenna with reflector to enhance isolation," *IEEE Transactions on Antennas and Propagation*, Vol. 63, No. 4, 1873–1877, 2015.
6. Liu, L., S. W. Cheung, and T. I. Yuk, "Compact MIMO antenna for portable devices in UWB applications," *IEEE Transactions on Antennas and Propagation*, Vol. 61, No. 8, 4257–4264, 2013.
7. Mathur, R. and S. Dwari, "A compact UWB-MIMO with dual grounded CRR for isolation improvement," *International Journal of RF and Microwave Computer-Aided Engineering*, Vol. 29, Art no. e21500, 2019.
8. Deng, J. Y., L. X. Guo, and X. L. Liu, "An ultra-wideband MIMO antenna with a high isolation," *IEEE Antennas and Wireless Propagation Letters*, Vol. 15, 182–185, 2016.
9. Khan, M. K., Q. Feng, and Z. Zheng, "Experimental investigation and design of UWB MIMO antenna with enhanced isolation," *Progress In Electromagnetics Research C*, Vol. 107, 287–297, 2021.
10. Sarkar, D., K. Sarkar, and K. Saurav, "A compact microstrip-fed triple band-notched UWB monopole antenna," *IEEE Antennas and Wireless Propagation Letters*, Vol. 13, 396–399, 2014.

11. Modirkhazeni, A., P. Rezaei, and I. A. Lafmajani, "Compact UWB antennas with inverted E- and F-shaped slots for bandnotch characteristics," *Progress In Electromagnetics Research Letters*, Vol. 56, 107–113, 2015.
12. Sharbati, V., P. Rezaei, and M. M. Fakhrian, "Compact planar UWB antenna with enhanced bandwidth and switchable band-notch function for WLAN and DSRC," *IETE Journal of Research*, Vol. 63, No. 6, 805–812, 2017.
13. Kuamr, A., A. Q. Ansari, B. K. Kanaujia, J. Kishor, and S. Kumar, "An ultra-compact two-port UWB-MIMO antenna with dual band-notched characteristics," *International Journal of Electronics and Communications (AEÜ)*, Vol. 114, Art no. 152997, 2020.
14. Du, C. and G. Jin, "A compact CPW-fed band-notched UWB-MIMO flexible antenna for WBAN application," *Journal of Electromagnetic Waves and Applications*, Vol. 35, No. 8, 1046–1058, 2021.
15. Luo, S., D. Wang, Y. Chen, E. Li, and C. Jiang, "A compact dual-port UWB-MIMO antenna with quadruple band-notched characteristics," *International Journal of Electronics and Communications (AEÜ)*, Vol. 136, Art no. 153770, 2021.
16. Zhang, J., L. Wang, and W. Zhang, "A novel dual band-notched CPW-fed UWB MIMO antenna with mutual coupling reduction characteristics," *Progress In Electromagnetics Research Letters*, Vol. 90, 21–28, 2020.
17. Sampath, R. and K. T. Selvan, "Compact hybrid Sierpinski Koch fractal UWB MIMO antenna with pattern diversity," *International Journal of RF and Microwave Computer Aided Engineering*, Vol. 30, Art no. e22017, 2020.
18. Masoodi, I. S., I. Ishteyaq, K. Muzaffar, and M. I. Magray, "A compact band notched antenna with high isolation for UWB MIMO applications," *International Journal of Microwave and Wireless Technologies*, 1–7, 2020.
19. Vyas, K. and R. P. Yadav, "Planar suspended line technique based UWB-MIMO antenna having dual-band notching characteristics," *International Journal of Microwave and Wireless Technologies*, 1–10, 2020.
20. Li, D. H., F. S. Zhang, G. J. Xie, H. Zhang, and Y. Zhao, "Design of a miniaturized UWB MIMO Vivaldi antenna with dual band-rejected performance," *IEICE Electronics Express*, Vol. 17, No. 16, 1–6, 2020.
21. Thakur, E., N. Jaglan, and S. D. Gupta, "Design of compact triple band-notched UWB MIMO antenna with TVC-EBG structure," *Journal of Electromagnetic Waves and Applications*, Vol. 34, No. 11, 1601–1615, 2020.
22. Banerjee, J., A. Gorai, and R. Ghatak, "Design and analysis of a compact UWB MIMO antenna incorporating fractal inspired isolation improvement and band rejection structures," *International Journal of Electronics and Communications (AEÜ)*, Vol. 122, Art no. 153274, 2020.
23. Kumar, J. P. and G. Karunakar, "Compact UWB-MIMO triple notched antenna for isolation reduction," *Wireless Personal Communications*, Vol. 115, 2113–2125, 2020.
24. Balanis, C. A., *Antenna Theory, Analysis and Design*, John Wiley & Sons, New York, 1997.
25. Chandel, R., K. Rambabu, and A. K. Gautam, "Design and packaging of an eye-shaped multiple-input-multiple-output antenna with high isolation for wireless UWB applications," *IEEE Transactions on Components, Packing and Manufacturing Technology*, Vol. 8, No. 4, 635–642, 2018.